Tellus (1995), 47A, 638–655
Printed in Belgium – all rights reserved

TELLUS
ISSN 0280–6495

An objective climatology of mobile troughs in the northern hemisphere

By RANDY J. LEFEVRE* and JOHN W. NIELSEN-GAMMON, *MS 3150, Department of Meteorology, Texas A & M University, College Station, Texas 77843-3150, USA*

(Manuscript received 2 September 1994; in final form 2 January 1995)

ABSTRACT

This paper introduces a technique to identify and track midtropospheric mobile troughs. Mobile troughs are objectively identified as maxima in the transport of geostrophic curvature vorticity. A 20-year climatology of mobile trough genesis and termination regions is constructed by applying the method to National Meteorological Center 500 mb geopotential height data. The objective tracking results are compared to Sanders' (1988) climatology of mobile troughs on the 552 dam contour. The objective method was shown to be more consistent and accurate than Sanders' subjective method, and therefore, determined to be superior in tracking midtropospheric mobile troughs. The mean lifespan of troughs over the 20-year dataset was 5.3 days and the maximum lifespan was 44 days. The geographical shape of the trough genesis and termination regions are associated with the orography. The three preferred genesis regions are north-central North America, the Mediterranean Sea, and southeast Asia. The three preferred termination regions are the extreme eastern Pacific Ocean, the Mediterranean Sea, and southwest Asia. Trough genesis regions tend to be well upstream of major areas of wintertime surface cyclogenesis.

1. Introduction

When one examines midlatitude height or pressure fields, one finds a tendency for closed contours at the surface and open, wavy contours near the jet stream level. Synoptic meteorologists use the terms "short wave" and "long wave" to categorize the wave properties. Petterssen (1956, p. 138) stated: "In typical cases one finds about four to five major waves around the hemisphere and these are called the long waves, or Rossby waves, after Rossby who first investigated their principal properties. Superimposed upon these long waves one finds shorter waves (often of quite small amplitudes) traveling through the slowly moving train of long waves." Long waves are quasi-stationary, while short waves are mobile.

The study of mobile troughs is motivated by their abundance in the atmosphere and their relationship to cyclogenesis. Petterssen (1955) noted that cyclogenesis occurs when an area of upper-level positive (cyclonic) vorticity advection associated with a pre-existing trough becomes superimposed over a low-level baroclinic zone. Petterssen and Smebye (1971) called this form of cyclogenesis "Type B" to distinguish it from the traditional description of an instability growing simultaneously from small amplitude at upper and lower levels (Type A). Sanders (1986) and others have found that Type B cyclogenesis is predominant, and even the existence of Type A cyclogenesis is questioned by some.

Despite the crucial role played by upper-level mobile troughs in cyclogenesis, few have studied the observed development and maintenance of mobile troughs. The only published synoptic climatology of upper-level mobile troughs in the northern hemisphere was by Sanders (1988, hereafter S88), who subjectively tracked bends in the 500 mb 552 dam geopotential height contour. He found that the median life span of mobile

* Corresponding author.

troughs was 12 days, with one "hero" lasting for 57 days and traveling twice around the northern hemisphere. The average phase speed of the troughs was estimated at 14.3° longitude per day, which corresponds to 12 m s^{-1} at 40° N. Trough genesis occurred more often over land, usually over and downstream of major mountain barriers, and most troughs terminated over oceans.

The S88 study has helped spawn theoretical interest in upper-level mobile troughs. Recent studies include Staley (1988), Snyder and Lindzen (1988), Whitaker and Barcilon (1992a), Whitaker and Barcilon (1992b), Rivest et al. (1992), and Rivest and Farrell (1992). Ideas range from localized baroclinic instability to quasi-neutral modes triggered by favorably-configured initial disturbances. Also relevant to the problem of mobile trough generation is recent work by Orlanski and Katzfey (1991), Chang (1993), Orlanski and Chang (1993), and Orlanski and Sheldon (1993) showing that upper-level mobile troughs can be generated by the transfer of energy from upstream baroclinically-growing cyclones.

The S88 study suffers from two serious shortcomings. First, because the tracking algorithm is based on subjective, qualitative criteria, the results are sensitive to the person doing the tracking. It is possible that troughs may be sustained by a subjective bias toward continuity. Second, because troughs were required to exist on the 552 dam contour, the climatology is strongly weighted toward midlatitude mobile troughs and cannot distinguish between a trough which forms on the 552 dam contour and a trough which moves toward the 552 dam contour from higher or lower latitudes.

The purpose of the present study is to produce a synoptic climatology of upper-level mobile troughs over the northern hemisphere using an objective trough tracking algorithm. Results will be compared to S88 and to the characteristics of cyclones and bandpass wave activity.

2. Data

The 500 mb data used in this study consisted of National Meteorological Center (NMC) 12-hourly gridded analyses for the period 1969 through 1988. The data, taken from CD-ROM (Mass et al., 1987), is on the NMC Octagonal Grid, a polar stereographic projection centered at the North Pole. The grid spacing varies from approximately 450 km at the pole to approximately 200 km at the equator. We focus on 500 mb to allow direct comparison with S88, and because the 500 mb level has been demonstrated to be an ideal single level for identifying upper-tropospheric mobile troughs that affect the lower troposphere.

3. Method

3.1. Objective trough identification

The tracking of specific surface-based disturbances is typically performed by following specific pressure minima. The pressure extremum must attain a specific threshold amplitude, measured by the number of closed contours surrounding the minimum, and the tracking may be performed either subjectively (Petterssen, 1956; Zishka and Smith, 1980) or objectively (Alpert et al., 1990; Sinclair, 1994).

At 500 mb, vorticity would seem to be a natural choice, since synopticians often use vorticity to subjectively track troughs. Dean (1993) has tracked vorticity maxima to study trough mergers and fractures. However, this technique fails for the simple dynamical case of a one-dimensional barotropic Rossby wave propagating along a shear zone on an f-plane. No maxima or minima of vorticity can exist, despite the possibility of high-amplitude troughs with large positive vorticity advection (PVA) downstream.

Relative vorticity may be subdivided in natural coordinates into shear vorticity and curvature vorticity:

$$\zeta_g = -\frac{\partial V_g}{\partial n} + \frac{V_g}{R_s}. \qquad (1)$$

In the equation above ζ_g is geostrophic relative vorticity, V_g is the magnitude of the geostrophic wind, n is a distance measured in the direction normal to the flow, and R_s is the radius of curvature of the geostrophic flow. The use of curvature vorticity to identify troughs would potentially circumvent the problem discussed above. However, it was found that curvature maxima often corresponded to closed, stationary circulation centers, or were located well poleward of the jet core where the strongest PVA would be occurring.

Both difficulties are avoided if the geostrophic curvature vorticity is multiplied by the magnitude of the geostrophic wind. This produces a quantity which may be called Eulerian Centripetal Acceleration, or ECA:

$$\mathrm{ECA} \equiv \frac{V_g^2}{R_s}. \tag{2}$$

One interpretation of ECA is as the centripetal acceleration experienced by an air parcel following the instantaneous geostrophic streamlines. It can also be interpreted as the transport of curvature vorticity by the geostrophic wind, which would be located just upstream of regions of PVA. However, a dynamical interpretation is unnecessary; the purpose of (2) is to define a quantity whose maxima at 500 mb correspond one-to-one with those features a synoptician would subjectively identify as mobile troughs.

The use of a quasi-conserved quantity, such as Ertel's potential vorticity (PV) or quasi-geostrophic potential vorticity, for tracking troughs was considered and rejected. Since Rossby waves propagate along PV gradients, a given wavelike mobile trough cannot be tracked by following a particular air parcel with anomalously high PV. Also, a given trough may be associated with a PV anomaly at one level or several levels. However, the use of ECA provides a measure of trough significance, since a given PV anomaly must be sufficiently strong to affect the geostrophic wind field at 500 mb to be identified as a trough.

In Fig. 1, ECA maxima are compared to the 500 mb geopotential height field and to troughs on the 552 dam contour as identified and reported by S88. It is readily seen that troughs are rarely of maximum intensity along the 552 dam contour, based upon either ECA maxima or subjective interpretation. However, there is a one-to-one

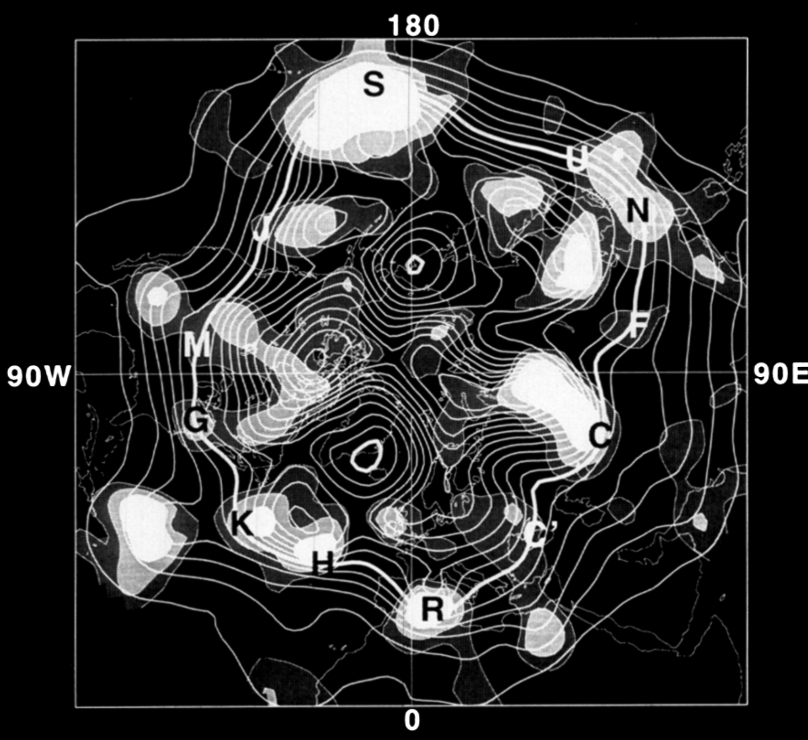

Fig. 1. 500 mb geopotential height (contours every 6 dam) and ECA (10^{-4} m s^{-2}) for 0000 UTC 22 February 1986. The trough labels correspond to Sanders (1988). The thick contour is the 552 dam contour. The regions with ECA greater than or equal to 1×10^{-4} m s^{-2} are shaded. The shading corresponds to contours of 1, 4, 10 and 30×10^{-4} m s^{-2}, respectively.

correspondence between 552 dam contour curvature maxima and nearby ECA maxima with magnitudes of 3.5×10^{-4} m s^{-2} or greater. For example, trough "K" over the central Atlantic Ocean is associated with a mobile trough whose maximum intensity is marked by ECA as being near the 540 dam contour. Thus, ECA can serve as a marker for the same troughs which S88 tracked as curvature maxima on the 552 dam contour. A critical advantage of ECA, though, is that it allows troughs to be followed even when they move north or south away from the 552 dam contour. Numerous intense troughs, such as the one over the British Isles or the southwestern United States, are captured by ECA but were missed by the S88 method.

3.2. *Trough tracking*

The mobile trough tracking portion of this technique evolved from an algorithm developed by Dean (1993) and was based on the premise that 500 mb mobile troughs can loosely be regarded as being steered by the 500 mb flow. The motion of a progressive Rossby wave, for example, would be due to the combination of the advective velocity and a smaller propagation velocity. Therefore, one would expect to find a given trough some distance downstream twelve hours later.

The tracking algorithm proceeds through a sequence of twelve-hourly 500 mb height analyses in chronological order, computing the geostrophic wind and ECA. At each analysis time, the gridded ECA data is searched for the occurrence of positive maxima of ECA, defined as a grid point whose ECA is larger than any of the eight surrounding grid points. Each potential maximum is then passed through a second check, which compares the ECA magnitude at the grid point to the magnitude of ECA in a circle surrounding the grid point at a radius equal to the grid spacing. The magnitude of the ECA along the circle was determined using bilinear interpolation. To be retained as a maximum the central value must be 1.0×10^{-4} m s^{-2} greater than the ECA on at least 65% of the circumference of the circle. In essence, a significant trough is one whose ECA is greater than 1.0×10^{-4} m s^{-2}, and is at least 1.0×10^{-4} m s^{-2} greater than the immediately adjacent area.

The threshold used in this study was based on a comparison between the objective method and subjectively analyzed 500 mb geopotential height charts. A lower threshold would include random, disorganized vorticity variations within areas of very weak flow, and a higher threshold would unnecessarily delay genesis events and speed termination events.

For each new maximum, the algorithm loops through all troughs present at the previous analysis time, using a method adapted from Dean (1993). A mean vector geostrophic wind is computed from the geostrophic wind at the location of the new maximum and the geostrophic wind at each previous trough location. This wind is used to compute a hypothetical motion for each previous trough. If the location of the new maximum agrees with the "expected" location (see Appendix) of any previous trough, a "hit" is recorded. After performing this calculation for all preexisting troughs, the following possibilities exist.

(1) No hits were recorded. The maximum is designated a new trough, and its position is recorded as a genesis event.

(2) One hit was recorded. The maximum is deemed to be the current position of the trough which recorded the hit. The track information for that trough is updated.

(3) One hit was recorded, but with a trough which had already been tracked onto the current analysis. This event is considered a splitting (fracture) trough. The maximum is designated a new trough, its genesis location is assigned to be the previous position of the trough which recorded the hit, and the current position of the new trough is the current position of the maximum.

(4) Two or more hits were recorded, but all were with troughs which had already been tracked onto the current analysis. The trough for which the first hit was found is deemed to have been the splitting trough, and the tracks are handled as in case 3.

(5) Two or more hits were recorded, with at least one of the troughs not yet tracked onto the current analysis. The maximum is deemed to be the current position of the as-yet-untracked trough with the longest lifespan of all such troughs recording a hit. The track information for that trough is updated.

After all maxima have been compared with the previous positions of trough tracks, there are typically one or more trough tracks which failed to be connected with a maximum in the current analysis.

Similarly, there may be one or more trough tracks originating in the current analysis, according to case 1. A final search is performed to see if any trough genesis events took place near the expected position of a trough which has terminated. This search covers a larger area than that used in the initial search; see the Appendix for details. Any trough whose termination was followed by a birth twelve hours later sufficiently near its expected position is deemed to have continued its existence; the genesis is negated and the genesis position becomes the trough's current position. In the case of conflict, the trough whose expected position is closest to the genesis event is preferred.

All completed trough tracks are subject to the following additional screening to eliminate weak troughs, short-lived troughs, and subtropical troughs: (1) Any troughs which fail to attain a magnitude of $4.0 \times 10^4\ \mathrm{m\,s^{-2}}$, which roughly correspond to the minimum magnitude of an S88 trough, are discarded. (2) Any troughs which fail to travel as far north as 30°N for at least one day (two 12-hourly maps) are discarded. (3) Any troughs which fail to survive for at least two days (four 12-hourly maps) are discarded. The term "unscreened trough" will be used to identify all troughs which pass test (3), without regard to tests (1) and (2).

When one or two analyses were missing, the expected advection distance was increased by the appropriate factor, and troughs were tracked across the data gap. However, within the data set were several gaps of three or more consecutive map times, across which it was deemed imprudent to attempt to objectively track mobile troughs. To avoid bias and to ensure that essentially all troughs stored prior to a data gap have a sufficient opportunity to live a full lifespan, any troughs which are generated within 15 days of such a gap were discarded. Also, since their times and places of births were unrecorded, any troughs which existed on the first analysis following a gap of three or more consecutive analysis times were discarded. As a result of the gaps and the measures taken because of them, troughs which formed on 4.7% of the days within the 20-year period are missing from this climatology. All event frequencies presented below have been corrected for this shortfall.

The authors validated the ECA trough tracking technique by comparing the ECA results over two weeks to subjective tracks constructed by several volunteer analysts. The ECA results compared favorably with the subjective results. The ECA method typically initiated and terminated mobile troughs within one 12-h time period of the subjective analyses. There did not seem to be an overall bias toward truncating or overextending the life span of the troughs. However, 4 troughs identified by the subjective analyses lasted for the entire 2-week period (none of the subjective analyses agreed on all 4 troughs), whereas only one trough tracked by the objective technique lasted that long. Each segment of the longest ECA track was successfully tracked by the subjective analyses, but the subjective analyses typically split and merged three different troughs to complete the longest ECA track.

4. Trough lifespans

The lifespan distribution of the 27,469 mobile troughs satisfying the criteria listed in Section 3 is shown in Fig. 2. Here, lifespan (in days) is half the number of consecutive twelve-hourly analyses on which a given trough was identified, and, in the case of a one or two analysis data gap, the number of analyses on which the trough was presumed to have existed. The average lifespan of a mobile trough was 5.3 days, and the median lifespan was 4 days. The seasonal variation of mean trough lifespan was insignificant. The winter and summer mean lifespans were 5.2 days. The spring mean lifespan was 5.3 days, and the fall was 5.4 days.

The distribution in Fig. 2 closely approximates a geometric distribution. The probability that a particular trough will cease to exist on the next analysis is 0.13 and is independent of how long that trough has existed so far. It therefore appears

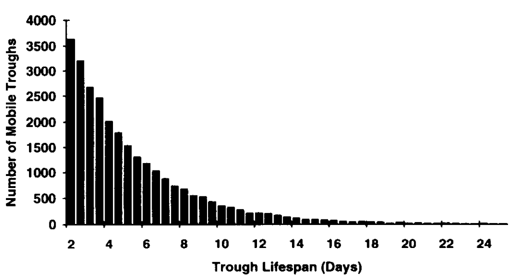

Fig. 2. Histogram of trough lifespan. The mean lifespan was 5.3 days, and the median was 4 days.

that upper-level mobile troughs are not subject to a life cycle of growth and decay of some typical length.

The lifespan of mobile troughs does depend on the place of birth of mobile troughs. For example, there is a strong dependence on latitude. Troughs forming near the pole exist for an average of 4 days, while troughs forming near 40° N exist for an average of 6 days. It is not known whether this effect is real or a consequence of the polar stereographic grid, which has a finer grid spacing at the equator. The smaller-scale troughs that form and remain closer to the equator can be resolved better than the smaller-scale troughs near the pole.

5. Comparison with Sanders' hero

Fig. 2 is in conflict with the S88 climatology. The S88 troughs had a median duration of twelve

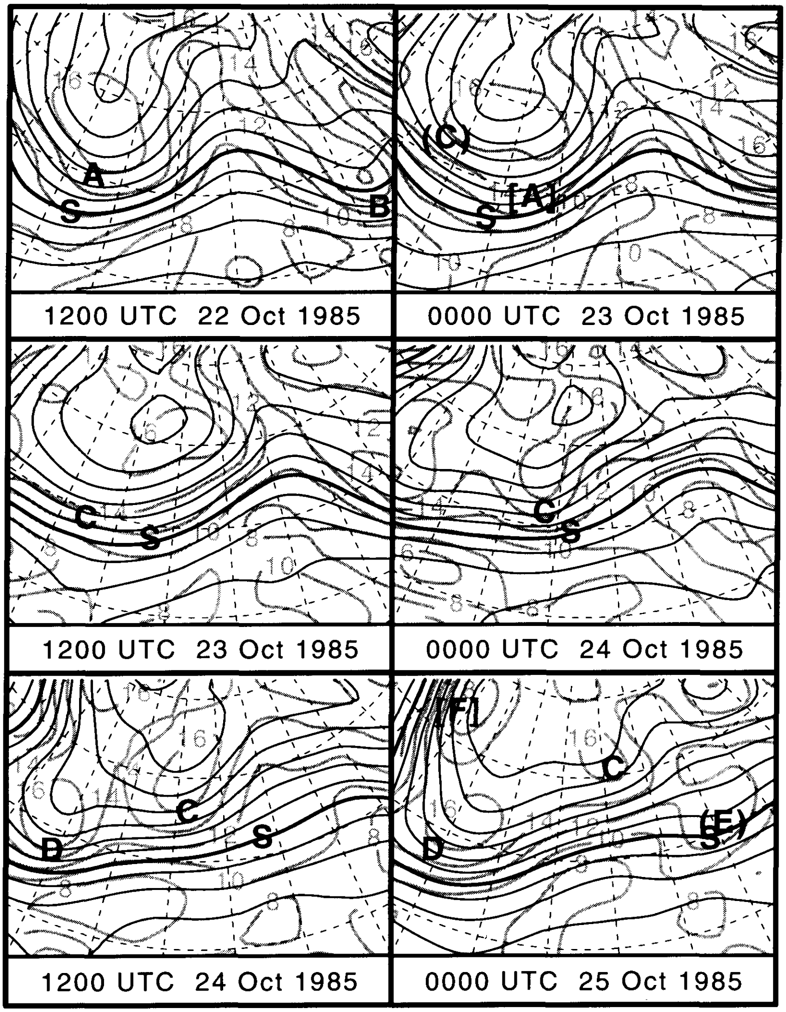

Fig. 3. Comparison of S88's longest-lived trough ("S") with objectively-tracked mobile troughs ("A" through "F"), 1200 UTC 22 October 1985 through 0000 UTC 25 October 1985. Height is contoured in black with an increment of 6 dam and absolute geostrophic vorticity is contoured in gray with an increment of $2.0 \times 10^{-5}\ s^{-1}$. The thick black contour identifies 552 dam geopotential height. The square brackets, [ ], indicate the trough terminated at this map time. The parentheses, ( ), indicate the trough formed at this map time. Latitude and longitude lines (dashed) are at 10° increments; the center bottom latitude and longitude are 40° N and 85° E, respectively.

days. In his six-month sample, Sanders identified five troughs which lasted 45 days or longer. In contrast, the longest-lived trough tracked by the objective method through twenty years of analyses lasted just 44 days. Although the objective method has been shown to identify features which are closely related to the S88 troughs, the difference between single-contour subjective tracking and objective tracking by ECA yields vastly different trough histories and lifespans.

To better understand the difference between objective and subjective tracking, the life history of the longest-lived trough in the S88 climatology (his trough "M") was examined with respect to the objective tracking of features associated with it. It was found that, although an objectively-tracked mobile trough could almost always be identified with the S88 trough, 14 different objectively-identified mobile troughs participated in its lifespan. In our opinion, of the thirteen discrepancies, the ECA objective tracking was superior in ten instances, the S88 subjective method was superior in one instance, and neither method was satisfactory in the remaining two. Two examples are presented below to illustrate the nature of the problem of trough tracking and to allow the reader to develop his or her own interpretation of the performance of each method.

Fig. 3 is a series of maps of 500 mb geopotential height and absolute geostrophic vorticity for a period one month into the lifespan of the S88 hero trough (which we denote with the letter "S"). In the first map, at 1200 UTC 22 October 1985, trough S is approaching central Asia. Sanders used only 0000 UTC analyses for this and other tracks; 1200 UTC analyses were not available to him for central Asia. The 1200 UTC plotted positions of the S88 trough have been interpolated from the 0000 UTC positions.

The ECA method identifies two mobile troughs in the map domain at 1200 UTC 22 October 1985. One, trough A, has been associated with trough S for about 2 days. The other, trough B, is exiting the domain to the east. Both troughs are associated with along-stream maxima of geostrophic vorticity, with positive vorticity advection (PVA) ahead and negative vorticity advection (NVA) behind.

12 h later, the region of PVA associated with trough A has become more elongated, and according to the objective method, trough A has split. The southern ECA maximum continues the track; the northern maximum, near 60° N, 95° E, is not assigned a letter because it failed to persist for two days and therefore never became an official trough. The square brackets indicate that trough A terminates on this map and could not be identified twelve hours later. Upstream, the parentheses indicate the location of birth of trough C. Trough C's birth appears to be of a common type: a closed vorticity center becomes elongated, with the original trough moving off to the northeast and a new trough forming in northwesterly flow behind it. While trough C is barely detectable at first, it eventually intensifies and satisfies the ECA strength criterion by 0000 UTC 24 October 1985. At that time, trough S is consistent with the position of trough C.

On the final map, at 0000 UTC 25 October 1985, trough S is collocated with a brand-new objectively-tracked trough, trough E. Trough C appears to have maintained good continuity as it moved off to the northeast, away from the 552 dam contour.

It appears that the objective ECA method has correctly identified the split and death of one trough and the birth of two others, events which were undetected by the S88 method. This process, in which one trough moves to the north or weakens while a new trough forms to its west, seems to have been a common source of error in the subjective method. In this instance, it is possible that the original trough A weakened as it approached the central Asian highlands and redeveloped as trough E on the lee slopes. However, as no continuous vorticity feature is detectable by eye during this hypothesized transit, it would be difficult to justify the statement that the 500 mb trough remained in existence during the transit.

The second example (Fig. 4) is taken from early in trough S's lifespan, as it first crossed the dateline. At 0000 UTC 7 October 1985, trough S is associated with the very intense trough I, which has just wrapped up and is undergoing north-south elongation. The objective method again splits the trough, with the southern lobe terminating at 0000 UTC 8 October 1985 near trough S and the northern lobe (unmarked, because it was short-lived) terminating twelve hours later. Meanwhile, a second region of strong PVA develops upstream, near 172° W at 1200 UTC 8 October 1985.

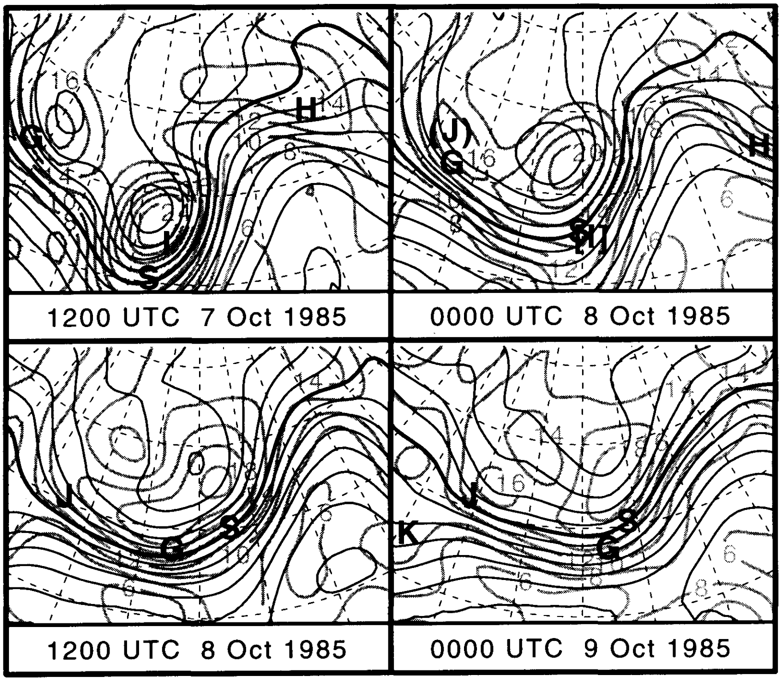

Fig. 4. Comparison of S88's longest-lived trough ("S") with objectively-tracked mobile troughs ("G" through "K"), 0000 UTC 7 October 1985 through 1200 UTC 8 October 1985. Heights, absolute vorticity, and trough labels are as in Fig. 3. Latitude and longitude lines (dashed) are at 10° increments; the center bottom latitude and longitude are 40° N and 170° W, respectively.

The objective method identifies this second region with the continuation of trough G. An alternative interpretation is that trough J, which supposedly split from trough G, is legitimately the continuation of trough G, and that the second region of PVA is actually a new trough. However, this PVA is not associated with the original trough I; that trough, and the PVA ahead of it, can be tracked from 180° at 1200 UTC 7 October 1985 to 170° W at 0000 UTC 8 October 1985 and to 160° W at 1200 UTC 8 October 1985. We conclude from this example that the S88 tracking was in error, and that the objective method selected one of the two available interpretations consistent with the data.

These two examples are representative of situations in which the objective method can have difficulty: a trough passing over high orography, a trough approaching a stationary region of anticyclonic curvature (not shown), and a trough splitting. We believe that the objective method tended to arrive at a defensible solution in most cases, while the S88 method clearly failed to track mobile troughs properly.

Notice that, in Fig. 4, a succession of troughs with an average wavelength of 1500–2000 km are tracked by the ECA method through a long-wave stationary trough. The use of the NMC Octagonal Grid analyses forces an effective short-wavelength cutoff for mobile troughs, since features with wavelengths shorter than about 1000 km cannot be represented in the analyses. Conversely, the use of a vorticity-based identification tool effectively eliminates long-wavelength features such as the stationary trough.

The life history of the longest-lived objectively-tracked trough was also closely examined. It was found that the objective technique appeared to switch from one trough to another three times during the 44-day track. During 30 consecutive days of tracking, the objective and subjective tracks agreed, so it seems likely that mobile troughs can survive as entities for a month or longer.

6. Inhomogeneities in the tracking statistics

Fig. 5 is a graph of mean unscreened trough lifespan as a function of time. In this figure, all troughs tracked for at least two days are included, whether or not they achieved minimum intensity or existed north of 30° N. While one might expect, or hope, that the trough statistics would remain stable from year to year, there is a strong tendency for longer-lived mobile troughs during the latter years of the 20-year dataset. At several points, there appear to be large, abrupt shifts in the mean lifespans.

The three largest discontinuities correspond to three of the seven changes made in the final analysis procedures at NMC during this period (Dey, 1989; Shuman, 1989). In September 1974, NMC switched from a Cressman analysis scheme to a Hough analysis. At that time, mean lifespans increased from 4.0 days to 4.3 days, and an apparent annual cycle in mean lifespan was eliminated. In September 1978, the Hough analysis was dropped in favor of optimal interpolation, and mean lifespans dropped back down to 4.0 days. Finally, in May 1980, the assimilation model was changed from a 9-layer finite-difference model to a 12-layer spectral model, and mean lifespans increased to 4.7 days.

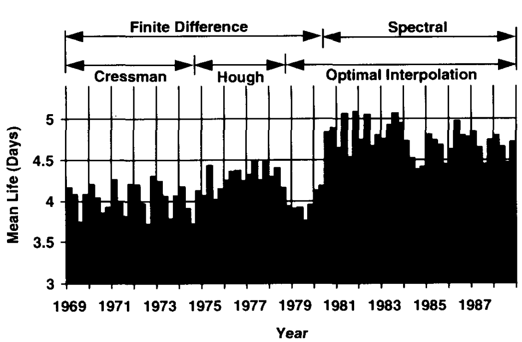

Fig. 5. A graph of mean lifespan of unscreened troughs (in days) versus time. Each column represents three months. The labels at the top identify the different procedures used by the National Meteorological Center (NMC) for the analyses. Note the seasonal variation within each year and the obvious differences in mean trough lifespan as the numerical analysis scheme changed.

Despite the inhomogeneities in the characteristics of the data set, the geographical distribution of mobile troughs and their genesis and termination locations remained remarkably stable in middle and high latitudes. Fig. 6 compares the frequency of occurrence of objectively-tracked unscreened mobile troughs on twelve-hourly analyses for the periods before and after the switch from a finite-difference model to a spectral model. Note that Fig. 6 is not a climatology of trough tracks, and will be biased against regions where the mean flow is stronger and troughs tend to be farther apart, such as the North Pacific. Figure 6 may be compared directly to cyclone frequencies such as those shown by Petterssen (1956).

Both maps share regions of high trough frequency over the North Pacific, North America, and North Atlantic. The consistency over the oceans is reassuring, and suggests that the presumed poorer quality of the early oceanic analyses has not seriously biased the statistics. Areas of low trough frequency correspond very closely to areas with the highest orography: the Tibetan Plateau, Greenland, and the Rocky Mountain Cordillera. These low-frequency areas will also appear as unlikely locations for trough genesis or termination.

Lower latitudes are dominated by regions of localized frequency maxima, which generally are much more prominent in the earlier portion of the dataset. These areas include the Mediterranean, northern India, and southeastern Asia. These are plausible areas for the existence of mobile troughs, but the relative frequency of mobile troughs there is sensitive to the analysis technique and therefore cannot be established in this study. We presume that the more recent analyses are more reliable.

7. Trough genesis and termination

The rates of trough genesis and termination over the northern hemisphere throughout the twenty-year data set are shown in Fig. 7. The three most favored regions of mobile trough genesis (Fig. 7a) are over eastern Asia (Mongolia and northeastern

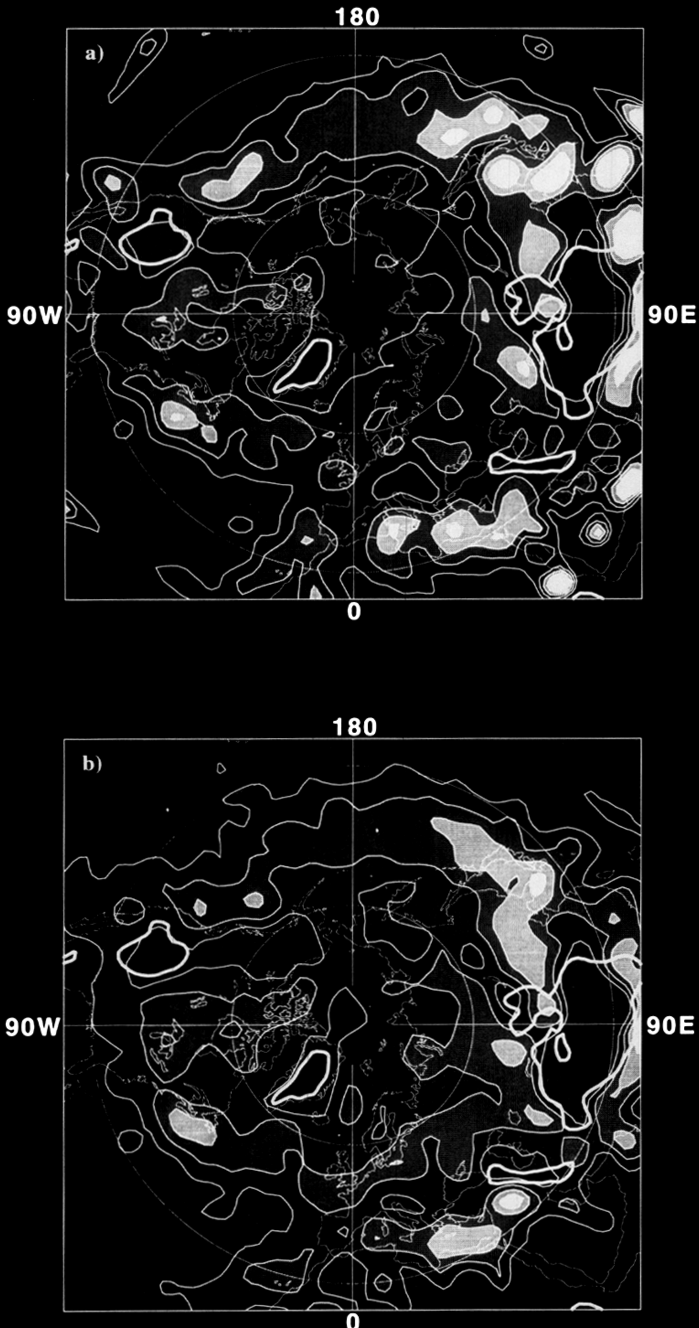

Fig. 6. (a) Frequency of trough appearance on 12-hourly 500 mb analyses for the period January 1969 through May 1980. (b) Frequency of trough appearance for the period June 1980 through December 1988. The single, unshaded contour is at 100 troughs per 10^6 km^2 per year. The contour shading represents 140, 180, 220 and 260 troughs per 10^6 km^2 per year, respectively. The thick contours encircle elevated terrain higher than 2000 m. The terrain data was taken from the National Meteorological Center's 2.5° resolution data set.

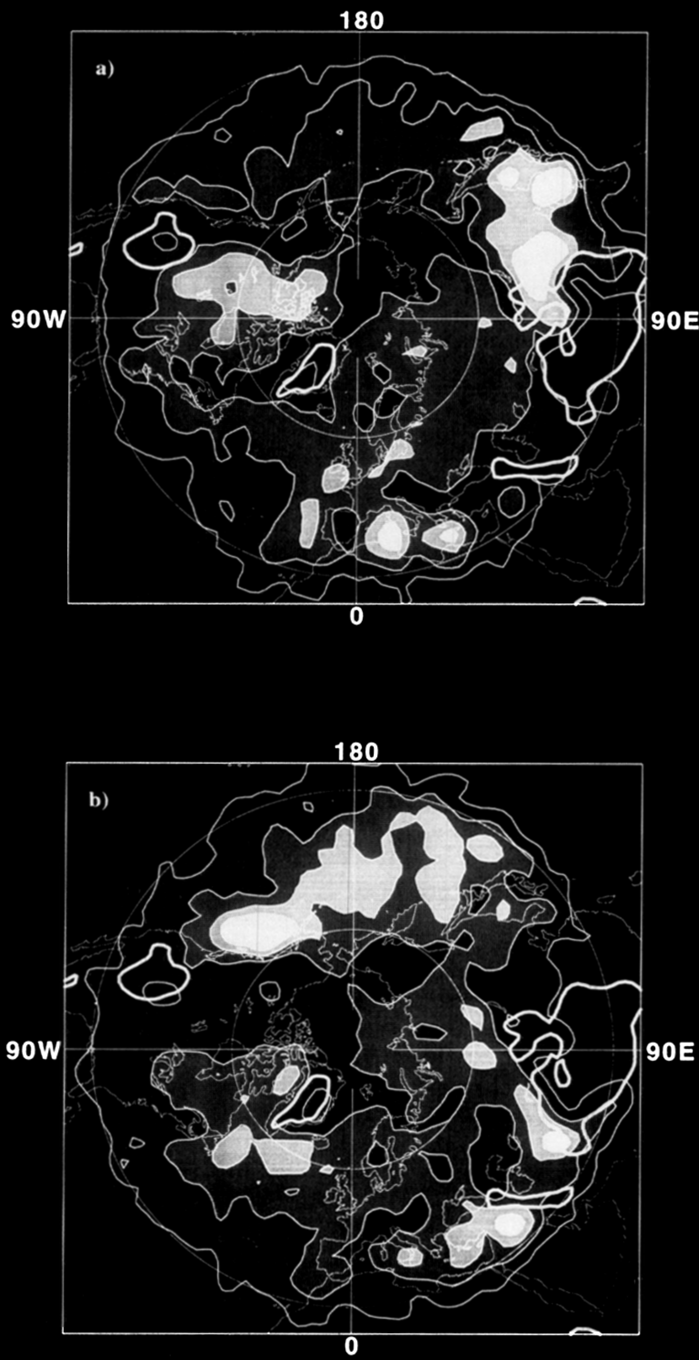

Fig. 7. (a) Frequency of trough genesis during all months throughout the twenty year dataset. (b) Frequency of trough termination during all months throughout the twenty year dataset. The solid contour shading represents 10, 15, 20 and 25 events per 10^6 km^2 per year, respectively. The thick contours encircle elevated terrain higher than 2000 m.

China), north-central North America, and the Mediterranean Sea. Genesis events are unlikely over eastern Russia and over major mountain ranges. Two of the preferred regions are upstream of the major oceanic storm tracks (Wallace et al., 1988).

S88 also identified the prominent genesis regions over Asia and North America. However, S88's Asian genesis area does not extend as far east and S88's North American genesis events are farther south. The favored region over the Mediterranean is not captured by S88 because the 552 dam contour rarely extends so far south. We hypothesize that S88's genesis maximum over eastern Europe is a consequence of troughs forming over the Mediterranean and northern Europe and subsequently affecting the 552 dam contour.

Mobile trough termination events (Fig. 7b) are very rare in the preferred genesis regions over North America and Asia. The region with the most frequent trough termination is over the eastern Pacific Ocean, upstream from a major mountain barrier. A second prominent termination region traces the western outline of the western Asian massif, composed of the Tien Shan, the Hindu Kush, the Himalayas, and the Tibetan Plateau. The eastern edges of the two termination regions almost exactly coincide with the western edges of the mountain barriers. Both of these termination regions are directly upstream of major genesis regions on the lee sides of these mountains. As seen in Fig. 6, relatively few troughs are tracked over these mountainous area. Either the objective method fails to track troughs as they pass over mountain barriers, or a large fraction of troughs which encounter mountain barriers are weakened and destroyed by them. The latter explanation is favored by the localized termination regions on the

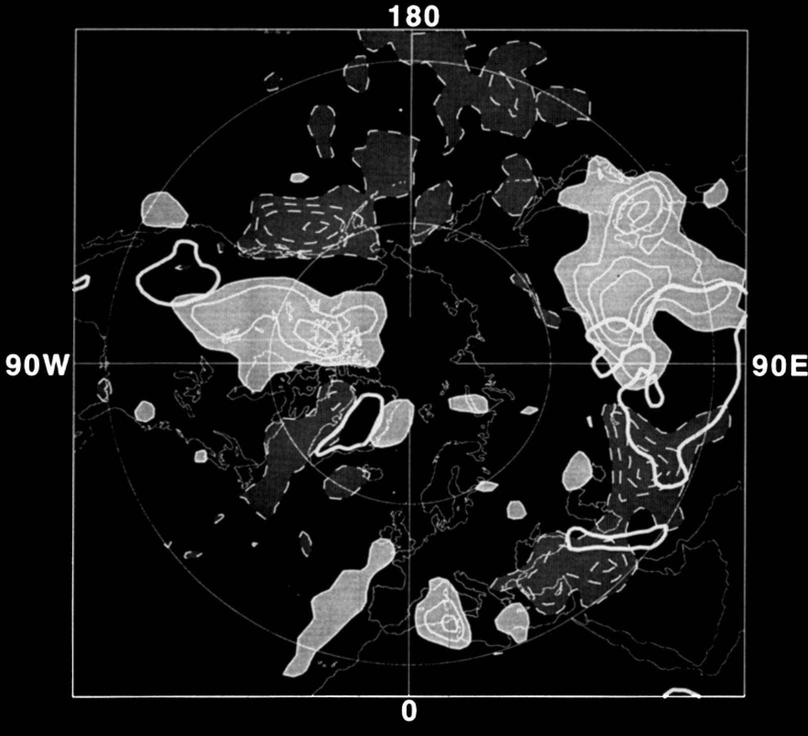

Fig. 8. Frequency of trough genesis minus trough termination for all months throughout the dataset. The darker shading and solid contours are areas where genesis exceeds termination. The solid contours represent values of 4, 8, 12 and 16 events per 10^6 km^2 per year, respectively. The lighter shaded areas and dashed contours are areas where trough termination exceeds genesis. The dashed contours represent values of -4, -8, -12 and -16 events per 10^6 km^2 per year, respectively. The zero contour is not plotted. The thick contours encircle elevated terrain higher than 2000 m.

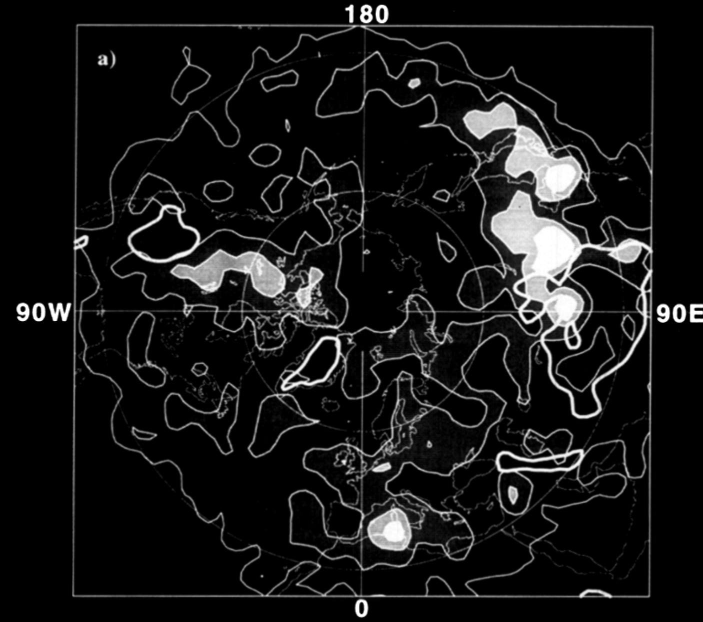

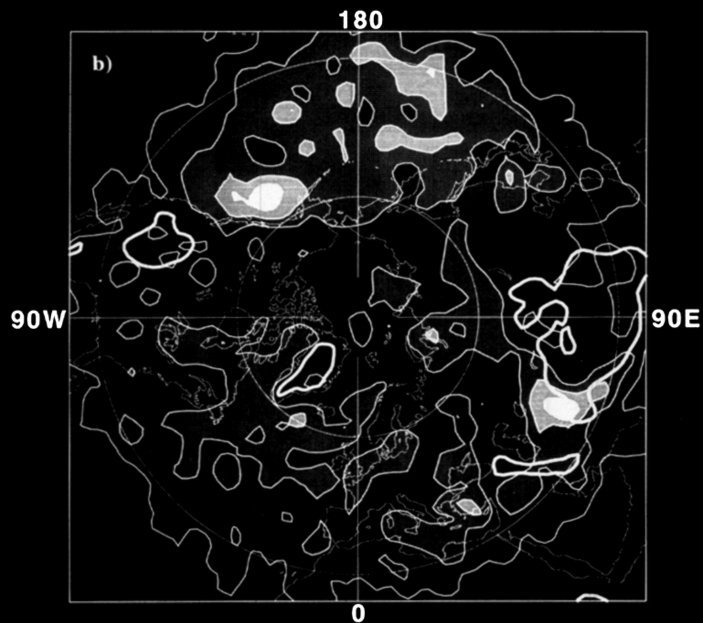

Fig. 9. (a) Frequency of trough genesis during winter (DJF) throughout the 20-year dataset. (b) Frequency of trough termination during winter (DJF) throughout the 20-year dataset. The solid contours represent 3, 5, 7 and 9 events per 10^6 km^2 per season, respectively. The thick contours encircle elevated terrain higher than 2000 m.

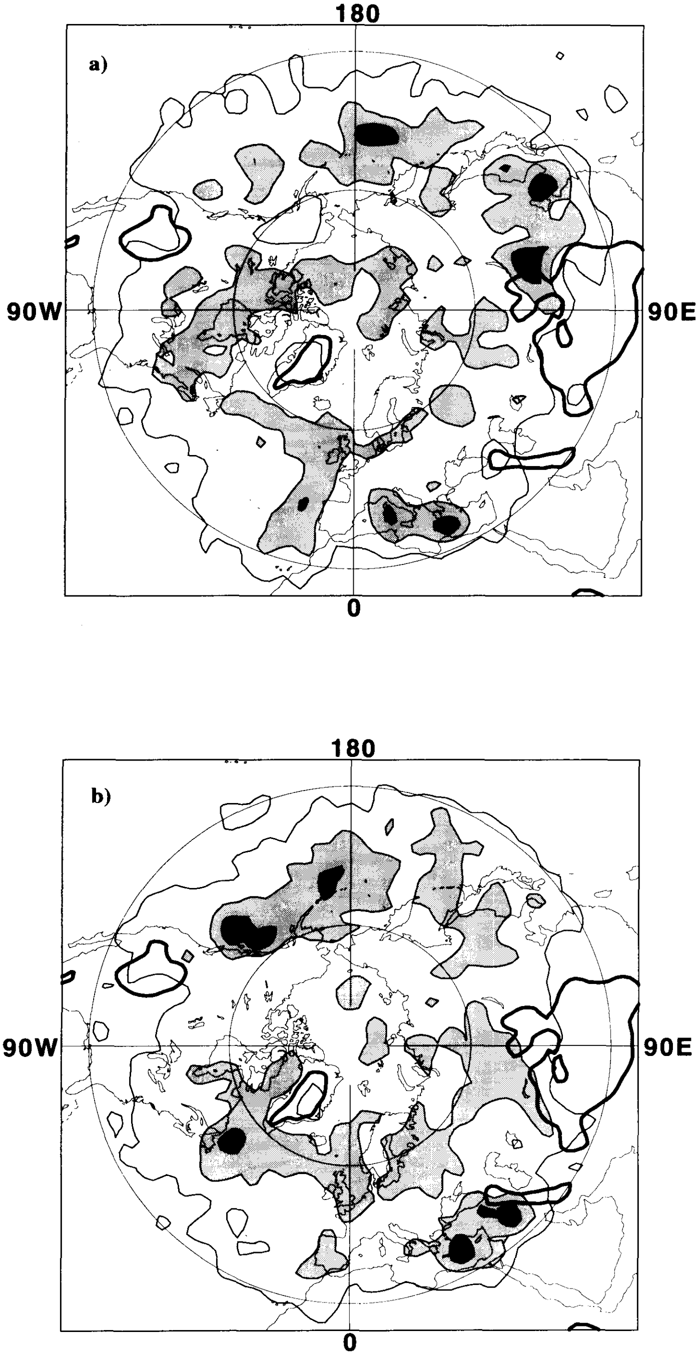

Fig. 10. (a) Frequency of trough genesis during summer (JJA) throughout the 20-year dataset. (b) Frequency of trough termination during summer (JJA) throughout the 20-year dataset. The contours represent 3, 5, 7 and 9 events per 10^6 km^2 per year. The thick contours encircle elevated terrain higher than 2000 m.

windward side of mountain ranges and the much broader generation regions beyond the lee.

Undoubtedly, as mentioned in Section 5, some troughs are inappropriately lost as they pass over stationary long-wave ridges, where the large-scale flow is curved anticyclonically. This would contribute to the termination region in the eastern Pacific, as troughs approach the climatological ridge in the geopotential height field along the west coast of North America. Except for an underestimate of termination events at low and high latitudes, the distribution of trough terminations in S88 agrees with the major termination features found here.

Fig. 8 shows the excess of genesis events over termination events per year. In general, as found by S88, genesis events are favored over land and termination events are favored over oceans. Trough genesis is preferred upstream of oceanic storm tracks, while trough termination is favored within and downstream of oceanic storm tracks. In addition, an area of preferred termination over western Asia is downstream of an area of preferred genesis over the Mediterranean Sea. Also, genesis events are favored over the extreme eastern Atlantic Ocean and off the southwestern coast of the United States. The eastern Atlantic generation region conflicts with S88, which found that the eastern Atlantic was dominated by a preferred termination region over and west of Europe. A similar pattern was also found by Dean (1993), who performed an objective climatology of 500 mb absolute vorticity centers.

The overall seasonal trough genesis patterns are similar to each other, and with the 20-year genesis patterns. In winter (Fig. 9) the same prominent areas of genesis and termination are found as in the charts including all months (Fig. 7). One difference is over the Pacific, where during winter, troughs tend to be generated in a narrow band between 30° N and 45° N. Termination events continue to be broadly distributed over the Pacific, but tend to be farther north than generation events. Also, both genesis and termination activity is enhanced over the south-central United States. The southward migration of trough activity is consistent with the seasonal migration of the strongest westerly winds.

In summer (Fig. 10) both genesis and termination events are more rare. Since trough lifespans are similar in the two seasons, troughs themselves must be rarer during summer. While the eastern Asian and Mediterranean genesis regions remain, the North American genesis region is weaker and displaced farther east. Two new prominent genesis regions appear, one over the central North Pacific and the other over the eastern Atlantic. There is little overlap with the area of wintertime genesis over the Pacific, suggesting that the broadness of the genesis pattern in the overall statistics is a consequence of averaging over a variety of jet positions. The termination region upstream of the western Asia massif is lost in summer, most likely as a consequence of the jet stream being farther north.

8. Summary and discussion

A method of objectively identifying midtropospheric mobile troughs has been developed and applied to twenty years of 500 mb analyses. The technique uses the product of the geostrophic curvature vorticity and the geostrophic wind speed, here called the Eulerian Centripetal Acceleration (ECA), to identify troughs, and estimates the motion of troughs from the 500 mb steering flow. This method was shown to be superior to the subjective curvature-of-contour technique of S88 in tracking features in the 500 mb vorticity field.

Mobile trough lifespans were found to obey a geometric distribution: the probability of a trough surviving to the next analysis was independent of the age of the trough. Lifespans were in general much shorter than S88 reported, with the longest-lived trough objectively tracked for 44 days. The median lifespan of "significant" mobile troughs was 4 days.

Mobile troughs appeared to follow preferred tracks, more frequently appearing over the storm track areas of the oceans and over the northern continents and the Mediterranean. Mobile troughs were rarely found over areas of high orography. The most likely area to find a trough north of 30° N was over the Yellow Sea, upstream of the major surface cyclone intensification region over the Pacific.

These frequency maps cannot be directly compared to counts of cyclone tracks passing through grid boxes, but they are comparable to the earlier climatologies of surface cyclone frequencies reported by Petterssen (1956) and Klein (1957). Over both the Atlantic and the Pacific, the axis of maximum trough frequency is displaced south of the axis of maximum cyclone frequency, probably because the cyclone frequency counts include mature, stationary cyclones which tend to lie north of the main band of westerlies. Across low latitudes from the Mediterranean to southeast Asia, preferred locations of mobile troughs and surface cyclones coincide. Over North America, the trough frequency maps lack an area of maximum frequency along the axis of high frequency of surface (lee) cyclones.

The major difference between preferred areas of surface cyclogenesis and upper-tropospheric mobile trough genesis is over the western oceans. While these are preferred regions for surface cyclone formation and intensification, these areas are much less active at upper levels than the major centers for mobile trough formation over central Asia and central North America. This is consistent with observations that typical rapidly-deepening surface cyclones over western oceans are triggered by preexisting upper-level short waves of significant amplitude (Sanders, 1986; Wash et al., 1988). Indeed, as found by S88, there is a robust tendency for mobile troughs to form over land and dissipate over water, with the notable exception of troughs which terminate on the upwind side of the Tibetan Plateau.

The eastern Asia trough genesis region is active year-round. Except for the relative lack of trough genesis south of Japan, the genesis pattern closely corresponds to the preferred locations of surface cyclogenesis found by Chen et al. (1991). However, the year-round activity over Mongolia contrasts with the behavior of surface cyclogenesis in that area, which is suppressed in winter (Whitaker and Horn, 1984, Chen et al., 1991). Over North America, cyclogenesis events form a narrow band in the lee of the mountains, while mobile trough genesis events are more broadly distributed downwind.

The above results are complementary to recent studies of bandpass variance and storm tracks. Both Blackmon et al. (1977) and Wallace et al. (1988) show the areas of high bandpass variance originating over eastern Asia at 500 mb and over Japan at 1000 mb. The bandpass variance maps show much less dependence on orography than the mobile trough frequency maps, doubtless due to mountains helping to amplify ridges even as they weaken troughs. The two prominent areas of genesis over the central continents are adjacent to and directly upstream of areas of 500 mb mobile disturbance amplification (Wallace et al., 1988). While we believe that dynamic processes in the genesis regions favor trough formation there, it is also possible that troughs that form there have a better chance of surviving at least two days because they quickly move into a region favoring intensification.

These results also complement the objective climatology of 500 mb cutoff cyclones and anticyclones performed by Bell and Bosart (1989). Not surprisingly, 500 mb closed low centers are most often found north of areas of high frequency of 500 mb mobile troughs. In middle and high latitudes, 500 mb closed low centers tend to form downstream of the major trough genesis areas, consistent with the model of troughs forming or intensifying within the storm track areas, and eventually becoming closed centers. In contrast, the areas of enhanced mobile trough formation south of 40° N in spring (not shown) neatly coincide with areas of cutoff low formation, implying that both processes occur simultaneously.

The ECA method does not explicitly screen out stationary troughs. Some of the troughs in the climatology actually became stationary for more than 24 h. Most of these troughs were found in the northeastern Pacific and the Gulf of Alaska (not shown), in an area with strong time-mean curvature of the 500 mb flow.

9. Acknowledgments

The authors wish to thank Lance Bosart and Devin Dean for providing their vorticity maximum identification and tracking software. We also thank Fred Sanders for his helpful thoughts and suggestions concerning mobile trough characteristics. This research was funded by the National Science Foundation under grant ATM-9218306 and by the United States Air Force.

10. Appendix

10.1. Advection region

To empirically determine the most probable area within which the trough would be expected to be found, a polar coordinate system is centered on the current location of a given trough exceeding the mobile trough threshold. For each trough found 12 h later, the mean geostrophic velocity is computed from the velocity of the new trough and the velocity of the original trough. The position of each new trough is then plotted on the polar diagram relative to the position each trough would have if it had been advected by the mean geostrophic velocity for twelve hours. If this process is repeated for all troughs in the 20-year data set, the result should consist of two contributions: a background trough count which represents the likelihood of finding a trough at any given point at any given time, and a non-random area of higher trough counts which represents the location to which each trough moves in 12 h.

The resulting plot is shown in Fig. 11 with the circular ring at the twelve-hour advective distance and the downstream axis oriented toward the right. It is not surprising to find the highest frequency of mobile troughs at distances less than or equal to the 12-h advective distance and approximately along the downstream direction. The winter season advection pattern (not shown) was similar to Fig. 11, but the summer season pattern (not shown) had more axial variation. The region of enhanced frequency is roughly elliptical, which was the shape of the advection region Alpert et al. (1990) used to objectively track surface cyclones.

To incorporate the advection region in the ECA tracking algorithm, radials extending from the center (origin) where constructed every 15°. A prescribed distance along each radial was used to determine if a point was inside or outside of the advective region. The outer margin of this advective region is shown by the thick line in Fig. 11.

10.2. *Final search for trough connection*

Occasionally, the objective tracking method would terminate one trough and begin another trough twelve hours later in a close proximity of the first trough's termination. Since the objective method did not find the second trough within the 12-h advection region, it thought the two troughs were separate. We investigated numerous occurrences of these termination-genesis couplets and found it reasonable to connect the new point to the old track. An additional search routine was developed to avoid this type of error, by broadening the search area when a trough terminates.

The final search algorithm searches the area around two key points. The first point is the location of the first trough's termination. The second point is near the center of the advective region downstream of the first trough's termination. To be considered for linkage the genesis must be within 500 km of the first key point or within one 12-h advective distance of the second point. The trough genesis nearest one of these points is connected to the first trough and the genesis is negated.

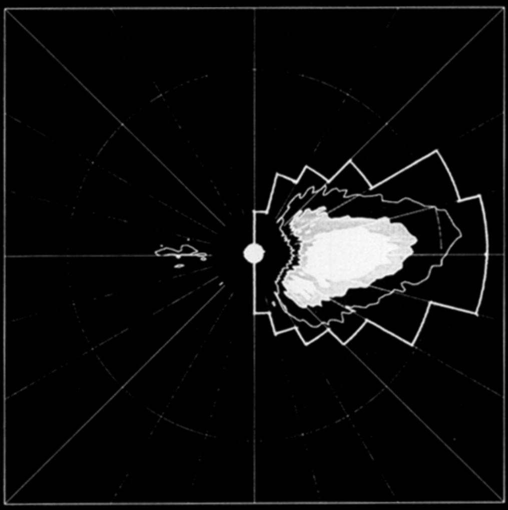

Fig. 11. A polar-coordinate schematic showing the shape of the 12-h advection region. The shaded area depicts the location of the highest 12-h advection frequency (normalized to 49,000 km^2). The contours represent 350, 600, 800 and 1000 troughs, respectively. The circle identifies the 12-h advection distance. The thick lines extending away from the origin outline the actual search region used in the objective tracking scheme.

REFERENCES

Alpert, P., Neeman, B. U. and Shay-El, Y. 1990. Climatological analysis of Mediterranean cyclones using ECMWF data. *Tellus* **42A**, 65–77.

Bell, G. D. and Bosart, L. F. 1989. A 15-year climatology of northern hemisphere 500 mb closed cyclone and anticyclone centers. *Mon. Wea. Rev.* **117**, 2142–2163.

Blackmon, M. L., Lau, N. C. and Mullen, S. L. 1977. An observational study of the northern hemisphere wintertime circulation. *J. Atmos. Sci.* **34**, 1040–1053.

Chang, E. K. M. 1993. Downstream development of baroclinic waves as inferred from regression analysis. *J. Atmos. Sci.* **50**, 2038–2053.

Chen, S. J., Kuo, Y. H., Zhang, P. Z. and Bai, Q. F. 1991. Synoptic climatology of cyclogenesis over East Asia. *Mon. Wea. Rev.* **119**, 1407–1418.

Dean, D. 1993. *A Northern Hemisphere climatology of 500 hPa trough merger and fracture.* Master's thesis, State University of New York at Albany, 234 pp.

Dey, C. H. 1989. The evolution of objective analysis methodology at the National Meteorological Center. *Wea. and Forecasting* **4**, 297–312.

Klein, W. H. 1957. *Principal tracks and mean frequencies of cyclones and anticyclones in the Northern Hemisphere.* Research Paper No. 40, U. S. Weather Bureau, 60 pp.

Mass, C. F., Edmon, H. J., Friedman, H. J., Cheney, N. R. and Recker, E. E. 1987. The use of compact discs for the storage of large meteorological and oceanographic data sets. *Bull. Amer. Met. Soc.* **68**, 1556–1558.

Orlanski, I. and Katzfey, J. 1991. The life cycle of a cyclone wave in the Southern Hemisphere. Part I: Eddy energy budget. *J. Atmos. Sci.* **48**, 1972–1998.

Orlanski, I. and Chang, E. K. M. 1993. Ageostrophic geopotential fluxes in downstream and upstream development of baroclinic waves. *J. Atmos. Sci.* **50**, 212–225.

Orlanski, I. and Sheldon, J. 1993. A case of downstream baroclinic development over western North America. *Mon. Wea. Rev.* **121**, 2929–2950.

Petterssen, S. 1955. A general survey of factors influencing development at sea level. *J. Meteor.* **12**, 36–42.

Petterssen, S. 1956. *Weather analysis and forecasting*, vol. 1. *Motion and motion systems.* McGraw-Hill, 428 pp.

Petterssen, S. and Smebye, S. J. 1971. On the development of extratropical cyclones. *Quart. J. Roy. Meteor. Soc.* **97**, 457–482.

Rivest, C., Davis, C. A. and Farrell, B. F. 1992. Upper-tropospheric synoptic-scale waves. Part I: maintenance as Eady normal modes. *J. Atmos. Sci.* **49**, 2108–2119.

Rivest, C. and Farrell, B. F. 1992. Upper-tropospheric synoptic-scale waves. Part II: maintenance and excitation of quasi modes. *J. Atmos. Sci.* **49**, 2120–2138.

Sanders, F. 1986. Explosive cyclogenesis over the west-central North Atlantic Ocean, 1981–1984. Part I: Composite structure and mean behavior. *Mon. Wea. Rev.* **114**, 1781–1794.

Sanders, F. 1988. Life history of mobile troughs in the upper westerlies. *Mon. Wea. Rev.* **116**, 2629–2648.

Shuman, F. G. 1989. History of numerical weather prediction at the National Meteorological Center. *Wea. and Forecasting* **4**, 286–296.

Sinclair, M. R. 1994. An objective cyclone climatology for the southern hemisphere. *Mon. Wea. Rev.* **122**, 2239–2256.

Staley, D. O. 1988. Baroclinic instability in the upper troposphere. *J. Atmos. Sci.* **45**, 3298–3304.

Snyder, C. and Lindzen, R. S. 1988. Upper-level baroclinic instability. *J. Atmos. Sci.* **45**, 2445–2459.

Wallace, J. M., Lim, G. H. and Blackmon, M. L. 1988. Relationship between cyclone tracks, anticyclone tracks and baroclinic waveguides. *J. Atmos. Sci.* **45**, 439–462.

Wash, C. H., Peak, J. E., Calland, W. E. and Cook, W. A. 1988. Diagnostic study of explosive cyclogenesis during FGGE. *Mon. Wea. Rev.* **116**, 431–451.

Whitaker, J. S. and Horn, L. H. 1984. Northern hemisphere extratropical cyclone activity for four mid-season months. *J. Climatol.* **4**, 297–310.

Whitaker, J. S. and Barcilon, A. 1992a. Type B cyclogenesis in a zonally varying flow. *J. Atmos. Sci.* **49**, 1877–1892.

Whitaker, J. S. and Barcilon, A. 1992b. Genesis of mobile troughs in the upper westerlies. *J. Atmos. Sci.* **49**, 2097–2107.

Zishka, K. M. and Smith, P. J. 1980. The climatology of cyclones and anticyclones over North America and surrounding ocean environs for January and July, 1950–77. *Mon. Wea. Rev.* **108**, 387–401.